Assimilation of remote sensing and hydrological data using adaptive filtering techniques for watershed modelling

Sat Kumar[1], M. Sekhar[1,*] and S. Bandyopadhyay[2]

[1]Department of Civil Engineering, Indian Institute of Science, Bangalore 560 012, India
[2]Earth Observation System, Indian Space Research Organization, Bangalore 560 094, India

The knowledge of hydrological variables (e.g. soil moisture, evapotranspiration) are of pronounced importance in various applications including flood control, agricultural production and effective water resources management. These applications require the accurate prediction of hydrological variables spatially and temporally in watershed/basin. Though hydrological models can simulate these variables at desired resolution (spatial and temporal), often they are validated against the variables, which are either sparse in resolution (e.g. soil moisture) or averaged over large regions (e.g. runoff). A combination of the distributed hydrological model (DHM) and remote sensing (RS) has the potential to improve resolution. Data assimilation schemes can optimally combine DHM and RS. Retrieval of hydrological variables (e.g. soil moisture) from remote sensing and assimilating it in hydrological model requires validation of algorithms using field studies. Here we present a review of methodologies developed to assimilate RS in DHM and demonstrate the application for soil moisture in a small experimental watershed in south India.

Keywords: Data assimilation, hydrological model, remote sensing, soil moisture.

Introduction

HYDROLOGICAL variables (e.g. soil moisture, evapotranspiration) play an important role in applications such as flood control, agricultural production and sustainable water resources management under hydroclimatic changes. These applications require an accurate prediction of hydrological variables spatially and temporally in a watershed/basin. Distributed hydrological models (DHM) can provide the desired variables at required resolution, and are useful for simulation of the anthropogenic effects, such as land use change, groundwater development and irrigation[1]. Remote sensing (RS) provides the data in the form of a squared grid, hence distributed hydrological models (DHM) with a similar grid structure are suitable to utilize this data. Input data and state variables, which can be assessed from the RS data cannot be explicitly included in the DHMs, so in order to fully utilize the RS data such models may require some adaptations[1]. Further, a particular problem in relation to the validation of distributed hydrological models is that, while spatial data such as topography, soil type and land cover are usually available as input data, spatiotemporal data such as vegetation indices, soil moisture and precipitation are often not available for calibration and validation[2,3]. Therefore, if distributed models are calibrated and validated only with a lumped variable of the entire catchment such as stream discharge, then the performance of the DHM is limited.

Remote sensing of variables such as precipitation, soil moisture and vegetation indices is one of the most promising techniques to bring spatiotemporal data into distributed hydrological models. RS provides an indirect measurement of hydrological variables and hence for extraction of the state variables, one has to resort to data retrieval algorithms. The use of remote sensing data in distributed hydrological models has been summarized for precipitation[4,5], snow[6,7], evapotranspiration[8,9], soil moisture[10,11] and hydrological modeling in general[12,13]. Principal focus and emphasis in the recent years, for example on soil moisture, has been on active and passive microwave methods[10,14,15]. The active methods, especially the synthetic aperture radar (SAR), can provide extremely good (<100 m) ground resolution from space[10]. However, the temporal resolution with the current satellites is less appropriate (~30 days) and distortions from surface roughness and vegetation in general limit the potential operational applications of the method to bare soil surfaces[16]. Further research on the use of multiple polarizations, frequencies, incident angles and temporal resolutions may lead to progress[17,18]. One of the major problems that is still unsolved is how to extend the remotely sensed surface signal (representing at a maximum the top 5 cm) to the root zone variable, although recent results in this field obtained by[16,19,20] are encouraging.

An additional complication in using the remotely sensed soil moisture in hydrological modeling is caused by the fact that both the remotely sensed and the mod-

*For correspondence. (e-mail: muddu@civil.iisc.ernet.in)

elled soil moisture are associated with several types of uncertainties which have to be accounted for. Data assimilation methods offer a way of combining input data and simulation results by taking into account their relative uncertainties, to update the state variable e.g. soil moisture with the remote sensed variable[21]. In this context, field studies can provide information on the natural distribution of soil moisture that will be of great importance for understanding the relationship between natural, model estimated and remotely sensed estimates of soil moisture distribution.

Data assimilation

The goal of data assimilation is to improve the state with the help of available measurements. In other words, the interest is in obtaining an improved estimate of the state ψ_k, at a fixed time t_k, as measurements become available. This could be the case, for example, if satellite provides indirect measurements of a hydrological variable at time t_k, the state at time t_k can be updated using the measurements up to time t_k. The process of updating state at time t_k using the measurements up to time t_k is called filtering. If the state at time $<t_k$ is updated using the measurements up to time t_k, this process is called smoothing. Figure 1 shows the smoothed estimate, analysed estimate ψ^a, model forecast or first guess ψ^f and prediction on time line, where measurements are available up to $k < 5$.

Assimilation can be performed in several ways. The simplest method is the direct insertion, but it does not take into consideration the fact that measured data is noisy and it updates state variable only locally where measurements are available. It does not update state where measurements are not available like in hydrology the interest is to update the root zone soil moisture given the surface soil moisture. There are several schemes better than direct insertion available for data assimilation such as 4D-Var, particle filter, Kalman filter, exponential filter, etc. Here as an example Kalman filter is illustrated, however any other filter can be applied in hydrology.

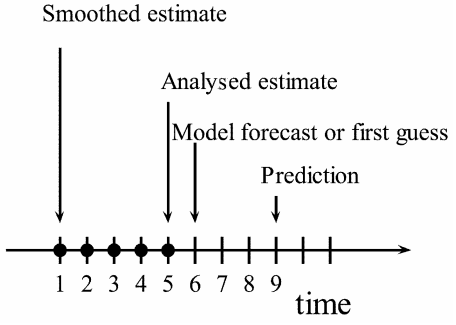

Figure 1. Time line showing the relationship between the *a posteriori*, *a priori*, smoothed, and predicted state estimates. [• represents the available measurements].

Discrete Kalman filter

The discrete Kalman filter provides a recursive way to estimate the state of the process in a way that minimizes the mean of the squared error[22]. It addresses the general problem of trying to estimate the state of a discrete-time controlled process that is governed by the linear stochastic difference equation given by

$$\psi_k^t = \mathbf{G}_{k,k-1}\psi_{k-1}^t + \mathbf{q}_{k-1}, \tag{1}$$

with a measurement that is

$$\mathbf{d}_k = \mathbf{M}_k\psi_k + \varepsilon_k. \tag{2}$$

Here ψ_k^t is the n dimensional true state, subscript k denotes the time step, $\mathbf{G}_{k,k-1}$ is the $(n \times n)$ dimensional linear transition matrix that relates the state at time t_{k-1} to time t_k, $\mathbf{M}_k$ is the $(n \times n)$ dimensional linear transition matrix that relates the measurements to state at time t_k, $\mathbf{q}_k$ is the n dimensional random vector which represents the process noise and ε_k is the n dimensional random vector which represents the measurement noise. These random noise vectors are assumed to be independent (of each other), white, and Gaussian with mean zero and may be written as

$$\overline{\mathbf{q}^f} = 0, \quad \overline{\mathbf{q}^f(\mathbf{q}^f)^T} = \mathbf{C}_{\psi\psi}^f,$$

$$\bar{\varepsilon} = 0, \ \overline{\varepsilon\varepsilon^T} = \mathbf{C}_{\varepsilon\varepsilon},$$

$$\overline{\mathbf{q}^f\varepsilon} = 0. \tag{3}$$

where overline represents the ensemble average, $\mathbf{q}^f$ denotes the unknown error in the forecast. The best estimate of ψ_k^t, written as ψ_k^a, based on the least square error criteria, and assuming ψ_k^a as an linear optimal combination of the *a priori* estimated state ψ_k^f and the observation $\mathbf{d}_k$ measured at the same time, can be written as

$$\psi_k^a = \psi_k^f + \mathbf{K}_k[\mathbf{d}_k - \mathbf{M}_k\psi_k^f]. \tag{4}$$

The forecasted (model) *a priori* estimate ψ_k^f is found by propagating ψ_{k-1}^a by the system equation. The Kalman gain matrix $\mathbf{K}_k$, can be found by minimizing the error covariance matrix $\mathbf{C}_{\psi\psi}$ w.r.t. the analysed state ψ_k^a, and can be written as

$$\mathbf{K}_k = \mathbf{C}_{\psi\psi}^f\mathbf{M}_k^T[\mathbf{M}_k C_{\psi\psi}^f\mathbf{M}_k^T + \mathbf{C}_{\varepsilon\varepsilon}]^{-1}, \tag{5}$$

now $\mathbf{C}_{\psi\psi}$ recursively can be written as:

$$\mathbf{C}_{\psi\psi}^a = [I - \mathbf{K}_k\mathbf{M}_k]\mathbf{C}_{\psi\psi}^f. \tag{6}$$

Extended Kalman filter (EKF)

If the relationship between state at two different time steps and between state and measurements at the same time step are not linear, there is a need to linearize them in order to use the Kalman filter. This linearization can be done using Taylor series, around the current estimate using the partial derivatives of the process and measurement functions to compute estimates even in the case of nonlinear relationships. Now process is governed by the nonlinear stochastic difference equation which can be expressed as

$$\psi_k^t = \mathbf{G}_{k,k-1}(\psi_{k-1}^t) + \mathbf{q}_{k-1}, \tag{7}$$

where the random variable **q** again represents the process noise and $\mathbf{G}_{k,k-1}(\psi)$ is the nonlinear model operator. In practice of course one does not know the noise at each time step. However, one can approximate the state vector without this information as

$$\psi_k^t = \mathbf{G}_{k,k-1}(\psi_{k-1}^a). \tag{8}$$

Here ψ_{k-1}^a is analysed state at previous time t_{k-1}. If governing equations are linearized about forecasted state, then the error covariance matrix $\mathbf{C}_{\psi\psi}^f$ at time t_k can be written as

$$\mathbf{C}_{\psi\psi}^f(t_k) \simeq \mathbf{G}'_{k,k-1}\mathbf{C}_{\psi\psi}^a(t_{k-1}) + \mathbf{G}'^T_{k,k-1} + \mathbf{C}_{qq}(t_{k-1}), \tag{9}$$

where

$$\mathbf{G}'_{k,k-1} = \left.\frac{\partial \mathbf{G}_{k,k-1}(\psi)}{\partial \psi}\right|_{\psi_{k-1}}. \tag{10}$$

It can be understood that in the EKF the distributions (or densities) of the various random variables are no longer normal after undergoing nonlinear transformation. The EKF only approximates optimality by linearization.

Ensemble Kalman filter (EnKF)

The ensemble Kalman filter (EnKF) is a suboptimal estimator, where the error statistics are predicted by using a Monte Carlo or ensemble integration[23]. The error covariances can be determined directly from the spread of the states in an ensemble at a certain point in time, instead of obtaining a value for the error covariance matrix calculated with an approximate linearized equation. Now the model error will be included in the ensemble perturbation, and its covariance is not explicitly needed anymore for the propagation of the state error covariances. Hence, the error covariance matrices for the predicted and the analysed estimate, namely $\mathbf{C}_{\psi\psi}^f$, $\mathbf{C}_{\psi\psi}^a$ can be defined in terms of the true state as

$$\mathbf{C}_{\psi\psi}^f = \overline{(\psi^f - \psi^t)(\psi^f - \psi^t)^T}, \tag{11}$$

$$\mathbf{C}_{\psi\psi}^a = \overline{(\psi^a - \psi^t)(\psi^a - \psi^t)^T}. \tag{12}$$

However, the true state is not known, so the ensemble covariance matrices can be defined around the ensemble mean $\overline{\psi}$,

$$(\mathbf{C}_{\psi\psi}^e)^f = \overline{(\psi^f - \overline{\psi^f})(\psi^f - \overline{\psi^f})^T}, \tag{13}$$

$$(\mathbf{C}_{\psi\psi}^e)^a = \overline{(\psi^a - \overline{\psi^a})(\psi^a - \overline{\psi^a})^T}. \tag{14}$$

Here superscript *e* denotes the estimate based on the ensemble integration. The ensemble of observations can be generated through the perturbation, expressed as

$$\mathbf{d}_j = \mathbf{d}_j + \varepsilon_j, \tag{15}$$

where *j* varies from 1 to *N*, the number of members in the ensemble. Next, covariance matrix of the measurements can be expressed as

$$\mathbf{C}_{\psi\psi}^e = \overline{\varepsilon\varepsilon^T}. \tag{16}$$

As the ensemble size approaches infinity, this matrix will converge to $\mathbf{C}_{\varepsilon\varepsilon}$. Now the Kalman gain can be written as

$$\mathbf{K}_k = (\mathbf{C}_{\psi\psi}^a)^f \mathbf{M}_k^T [\mathbf{M}_k (\mathbf{C}_{\psi\psi}^e)^f \mathbf{M}_k^T + \mathbf{C}_{\varepsilon\varepsilon}]^{-1}. \tag{17}$$

Adaptive filtering

The estimate of the state depends on error covariance matrices of the state and measurements. If the approximation of the error covariance matrices are not good enough, then the assimilation system will perform poorly. The approximation could be poor due to linearization of state, or finite number of ensembles, or due to change in the statistics of the model and measurement errors. The central idea behind adaptive filtering method is to update the error covariance matrices of the filter, to match the measurements. This is done by analysing the errors between the updated state and measurements, and errors between the updated estimate and analysed estimate, expressed as

$$\omega_k = \overline{\mathbf{d}_k - \mathbf{M}_k \psi_k^a}, \tag{18}$$

$$\nu_k = \overline{\mathbf{M}_k (\psi_k^a - \psi_k^f)}. \tag{19}$$

Here ω_k is analysis departure and ν_k analysis increment[24]. Based on the statistics of the analysis departure and

analysis increment, the error covariance can be updated as

$$\mathbf{C}^{e}_{\psi\psi}(t_{k+1}) = \alpha_k \mathbf{C}^{e}_{\psi\psi}(t_k), \tag{20}$$

$$\mathbf{C}^{e}_{\varepsilon\varepsilon}(t_{k+1}) = \beta_k \mathbf{C}^{e}_{\psi\psi}(t_k), \tag{21}$$

where α and β are estimated from the statistics of the analysis increment and departure[24].

Algorithm testing and field experiments

In this section the data assimilation theory discussed above has been demonstrated using the soil moisture model which is a module in DHMs. There are mainly three steps involved in this procedure: (i) model calibration in the watershed, (ii) retrieval of soil moisture from the backscatter coefficient, and (iii) assimilating backscatter coefficient into the soil moisture model. RS provides the indirect measurements of surface soil moisture (~5 cm), but the presence of surface roughness due to tilling practices, scattering by vegetation and type of soil affect the backscatter coefficient. To study the performance of the retrieval algorithm and data assimilation scheme in a watershed, for common types of crops and soils found in south India, experiments were carried out, which would be explained in the subsequent sections.

The Maddur experimental watershed

The Maddur watershed (12°30′N and 76°30′E) is located in the Kabini river basin approximately 20 km southwest of Gundulpet (in the Chamarajanagar district of Karnataka) along the National Highway (NH) to Sultan Battery (Waynad district, Kerala). The watershed runs along the northwest to south east covering a catchment area of 7.2 km^2. The watershed has semi-arid zone climate with a mean annual dominant south-west monsoon rainfall of 800 mm. The watershed is located close to the Bandipur National Park as its west boundary. There are mainly three types of soils in the watershed comprising black, red and rocky/weathered soils, as identified by the geophysical studies, which are representative of the soil types for granitic/gneissic lithology found in south India. Apart from it the stratification in each soil type is ascertained through field pits. The watershed comprises land use such as dense/closed forest, scrub forest, land with scrub, kharif crop, double crop and plantation classes. During kharif and rabi, crops such as marigold, sunflower, finger millet, maize, garlic, etc. are grown in various plots. The hourly rainfall, 15 min stream gauging and 15 min meteorological parameters suitable for computing potential evapotranspiration (PET) are recorded continuously through instrumentation installed in the watershed. The depth-wise soil moisture data was collected at three locations in all the three types of soils up to a depth of 2 m with sampling at depths of 10, 30, 50, 70, 90, 110, 130, 150, 170 and 190 cm.

Soil moisture model

Flow in the unsaturated porus media can be described by Darcy's law. Insertion of Darcy's law into continuity equation leads to the well-known Richards' equation[25]. In one dimension it can be expressed as

$$\frac{\partial \theta}{\partial t} = \frac{\partial}{\partial z}\left(K(h)\left(\frac{\partial h}{\partial z} - 1\right)\right) - S, \tag{22}$$

where θ is volumetric soil moisture content, z the elevation relative to a plane (positive downward), K the hydraulic conductivity, h the pressure head, S the sink term to account for root water uptake and t is time. Analytical solution of this nonlinear partial differential equation for the field boundary conditions is not available. So one has to discretize the equation into space and time using either finite difference or finite element methods. A soil moisture model based on the finite element method has been developed in the MATLAB using the pde (partial differential equation) toolbox. The model has been tested with the standard numerical solution available for infiltration and exfiltration dynamics in the presence of stratified soil layers. The generalized likelihood uncertainty estimation (GLUE) technique has been used for the calibration of the model. This approach allows for the possible equifinality (non-uniqueness, ambiguity or nonidentifiability) of parameter sets during the estimation of model parameters (inverse problem) in the overparameterised models[26]. Figure 2 shows the simulated and measured soil moisture profiles for various soils.

Data assimilation

To explore the capability of data assimilation in retrieving the root zone soil moisture from surface soil moisture, one synthetic experiment has been performed. In the synthetic experiment, the soil moisture is simulated for 200 days with synthetic parameters along with measured forcing (precipitation and potential evapotranspiration) in the field. Errors with normal distribution (mean zero and std. 2.5) are added to the simulated soil moisture to incorporate the effect of measurement error. Now with this noisy surface soil moisture, attempt has been made to retrieve the root zone (at 60 cm depth) soil moisture. Figure 3 shows the retrieved soil moisture at 20 and 60 cm depth with an assimilation frequency of 1, 12, 24 and 72 h. As can been seen from Figure 3, the retrieved root zone soil moisture is able to capture the dynamics but shows a bias with the actual truth. Generally data assimilation schemes

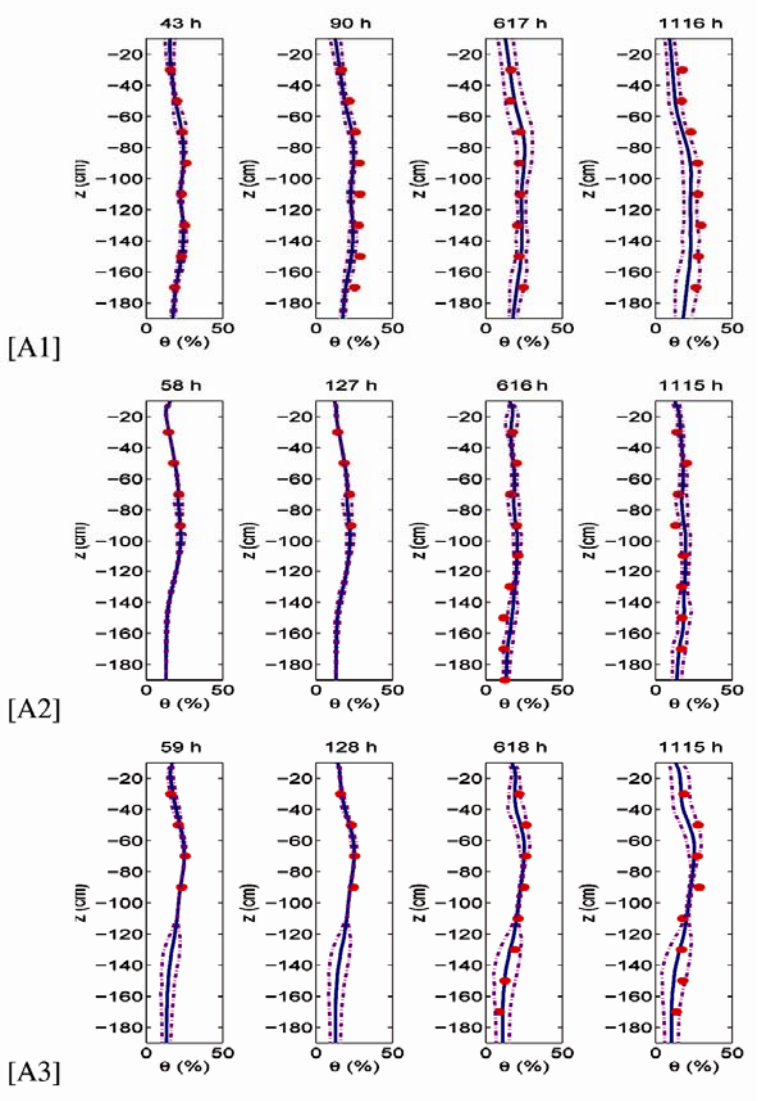

Figure 2. Simulation of soil moisture at A1 (black soil), A2 (red soil) and A3 (weathered soil). (Time 0 h – 10 October 2007, 00:00:00; Simulated (solid line), confidence interval (dashed line) and measured (filled circle)).

Table 1. Date, beam and incidence angle range for satellite images

Date	Beam	Incidence angle range (degree)
13 August 2008	IS6	39.1–42.8
20 August 2008	IS1	15.0–22.9
01 September 2008	IS6	39.1–42.8
05 September 2008	IS1	15.0–22.9

perform well in the case when measurements are given at some points well distributed in the model space. However in the present case since the measurements are only provided at the top boundary, results in a bias.

Surface soil moisture from RS

To study the retrieval algorithms of soil moisture from RS, 25 plots had been selected for monitoring soil moisture. These plots were in different types of soil, having different types of vegetation like marigold, sunflower, finger millet, maize, garlic, etc. and some were bare. Four campaigns have been carried out, to measure the surface soil moisture, soil roughness, water content in plants, simultaneously with the satellite pass. The satellite data were of ENVISAT with two polarizations HH and VV. Table 1 shows the details of the satellite images.

The first-order solution of the radiative transfer equation through a weak medium, neglecting the multiple scattering is called as 'water-cloud' model[27]. In this, backscattering is expressed as a linear combination of backscattering by vegetation and backscattering by soil, expressed as

$$\sigma_0 = \sigma^0_{\text{veg}} + \tau^2 \sigma^0_{\text{soil}}, \tag{23}$$

where σ^0_{soil} is the backscattering by the underlying soil and σ^0_{veg} is the backscattering by the vegetation, expressed as

$$\sigma^0_{veg} = A\cos\theta(1-\tau^2), \tag{24}$$

and τ^2 is the attenuation by the vegetation layer,

$$\tau^2 = \exp(-2Bm_v/\cos\theta). \tag{25}$$

The effect of the vegetation on the backscattered signal is thus represented by a single canopy variable, the water content of the canopy m_v (kg H_2O/m^2) and by two parameters, A and B, that are usually obtained from experimental data. The underlying soil contribution σ^0_{soil} can be evaluated from a surface scattering model or, more simply, from a linear function of its surface soil moisture m_s, expressed in dB units as[28,29]

$$\sigma^0_{soil} = C + Dm_s. \tag{26}$$

Here the parameters A and B are obtained from the experimental data, are kept constant for the dates 13 August 2008 and 20 August 2008, and for 1 September 2008 and 5 September 2008, assuming the small variations in the vegetation during this period. However, the parameters are different for the first and last two dates. The soil parameters C and D are also obtained from the experimental

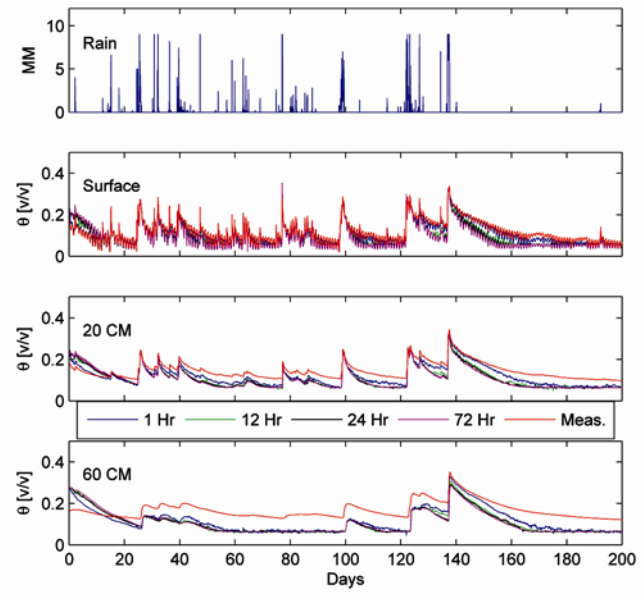

Figure 3. Rain and soil moisture at surface, 20 and 60 cm as retrieved by the ensemble Kalman filter.

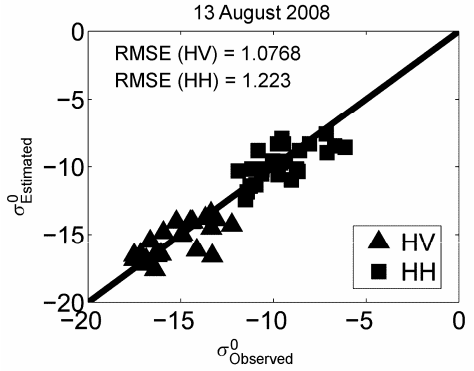

Figure 4. Observed vs calculated backscatter coefficient on date 13 August 2008.

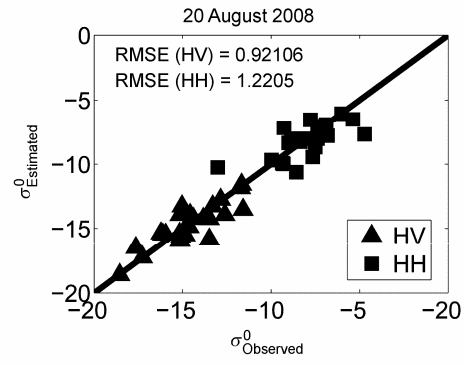

Figure 5. Observed vs calculated backscatter coefficient on date 20 August 2008.

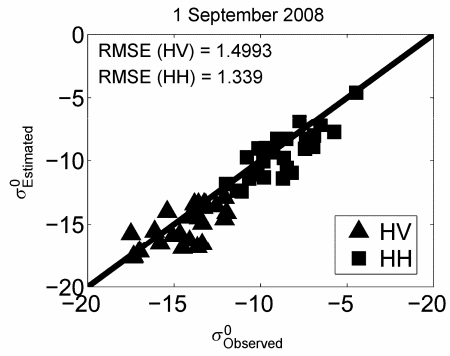

Figure 6. Observed vs calculated backscatter coefficient on date 1 September 2008.

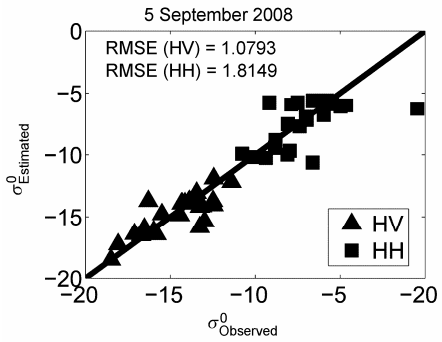

Figure 7. Observed vs calculated backscatter coefficient on date 5 September 2008.

data, which are kept constant for the entire period. The model shows a good relationship (RMSE (root mean squared error) < 1.8 db) between simulated backscatter coefficient and that estimated from the field experiments. Hence using this calibrated model, it is feasible to simulate the surface soil moisture for the entire watershed during the satellite pass. This surface soil moisture can be assimilated into the DHM to calibrate the model with the measured runoff in the watershed.

Conclusion

The data assimilation algorithms based on filtering methods have been summarized to incorporate RS data into hydrological models, especially when model and measurement equation are nonlinear. Application of the data assimilation algorithm has been shown for the retrieval of root zone soil moisture from noisy measurements of surface soil moisture. Though the predicted root zone soil moisture is able to capture the dynamics, a bias is observed. Updating frequency has no effect on the simulations. There is a need to remove this bias from the root zone soil moisture. The way to remove this bias can come either from the quasi-measurements of root zone soil moisture or any other hydrological variable that has information about the root zone soil moisture. The quasi-observation could be the root zone soil moisture under steady state condition of model for the given fluxes. Other remote sensing based variable such as vegetation indices (e.g. NDVI, TDVI) can be assimilated into the hydrological model, since vegetation indices are representative of soil moisture in the root zone.

1. Refsgaard, J. C. and Knudsen, J., Operational validation and intercomparison of different types of hydrological models. *Water Resour. Res*., 1996, **32**, 2189–2202.
2. Beven, K., How far can we go in distributed hydrological modelling? *Hydrol. Earth Syst. Sci*., 2001, **5**, 1–12.
3. Refsgaard, J. C., Parameterisation, calibration and validation of distributed hydrological models. *J. Hydrol*., 1997, **198**, 69–97.
4. Petty, G. W. and Krajewski, W., Satellite rainfall estimation over land. *Hydrol. Sci. J.*, 1996, **41**, 433–451.
5. Anagnostou, E. N., Overview of overland satellite rainfall estimation for hydro-meteorological applications. *Surv. Geophys*., 2004, **25**, 511–537.
6. Rango, A., Spaceborne remote sensing for snow hydrology applications. *Hydrol. Sci. J*., 1996, **4**, 477–494.
7. Jain, S. K., Goswami, A. and Saraf, A. K., Accuracy assessment of MODIS, NOAA and IRS data in snow cover mapping under Himalayan conditions. *Int. J. Remote Sensing*, 2008, **29**, 5863–5878.
8. Kustas, W. P. and Norman, J. M., Use of remote sensing for evapotranspiration monitoring over land surfaces. *Hydrol. Sci*., 1996, **41**, 495–516.
9. Agam, N., Kustas, W. P., Anderson, M. C., Li, F. and Colaizzi, P. D., Utility of thermal image sharpening for monitoring field-scale evapotranspiration over rainfed and irrigated agricultural regions. *Geophys. Res. Lett.*, 2008, **35**, L02402.
10. Jackson, T. J. and Schmugge, T. J., Remote sensing applications to hydrology: soil moisture. *Hydrol. Sci*., 1996, **41**, 517–530.
11. Moran, M. S., Christa, D., Peters-Lidard, Joseph, M. W. and McElroy, S., Estimating soil moisture at the watershed scale with satellite-based radar and land surface models. *Can. J. Remote Sensing*, 2004, **30**, 805–826.
12. Kite, G. W. and Pietroniro, A., Remote sensing applications in hydrological modelling. *Hydrol. Sci*., 1996, **41**, 563–591.
13. Boegh, E. *et al.*, Incorporating remote sensing data in physically based distributed agro-hydrological modelling. *J. Hydrol*., 2004, **287**, 279–299.
14. Lakshmi, V., Wood, E. and Choudhury, B., Evaluation of special sensor microwave/imager satellite data for regional soil moisture estimation over the red river basin. *J. Appl. Meteorol*., 1997, **36**, 1309–1328.
15. Dubois, P., Zyl, J. V. and Engman, T., Measuring of soil moisture with imaging radars. *IEEE Trans. Geosci. Remote Sensing*, 1995, **33**, 915–926.
16. Hoeben, R. and Troch, P., Assimilation of active microwave observation data for soil moisture profile estimation. *Water Resour. Res*., 2000, **36**, 2805–2819.
17. Dobson, M. and Ulaby, F., Active microwave soil moisture research. *IEEE Trans. Geosci. Remote Sens*., 1986, **24**, 2336.
18. Verhoest, N. E. C., Troch, P. A., Paniconi, C. and De Troch, F. P., Mapping basin scale variable source areas from multi-temporal remotely sensed observations of soil moisture behaviour. *Water Resour. Res*., 1998, **34**, 3235–3244.
19. Calvet, J.-C., Noilhan, J. and Bessemoulin, P., Retrieving the root-zone soil moisture from surface soil moisture or temperature estimates: a feasibility study based on field measurements. *J. Appl. Meteorol.*, 1998, **37**, 371–386.
20. Wigneron, J.-P. *et al.*, Soil moisture retrievals from bi-angular l-band passive microwave observations. *IEEE Trans. Geosci. Remote Sens*., 2004, **4**, 277–281.
21. Houser, P. R. *et al*., Integration of soil moisture remote sensing and hydrologic modelling using data assimilation. *Water Resour. Res*., 1998, **34**, 34053420.
22. Kalman, R. E., A new approach to linear filtering and prediction problems. *Trans. ASME. Ser. D.J. Basic Eng.*, 1960, **82**, 35–45.
23. Evensen, G., Sequential data assimilation with a nonlinear quasigeostrophic model using Monte Carlo methods to forecast error statistics. *J. Geophys. Res*., 1994, **99**, 10143–10162.
24. Reichle, R. H., Crow, W. T. and Keppenne, C. L., An adaptive ensemble kalman filter for soil moisture data assimilation. *Water Resour. Res*., 2008, **44**, W03423.
25. Celia, M., Bouloutas, E. and Zarba, R., A general mass conservative numerical solution for the unsaturated flow equation. *Water Resour. Res*., 1990, **26**, 1483–1496.
26. Beven, K., *Rainfall-Runoff Modelling. The Primer*, John Wiley, Chichester, 2001.
27. Attema, E. P. W. and Ulaby, F. T., Vegetation modelled as a water cloud. *Radio Sci*., 1978, **13**, 357–364.
28. Ulaby, F. T., Batlivala, P. P. and Dobson, M. C., Microwave backscatter dependence on surface roughness, soil moisture and soil texture: Part I – Bare soil. *IEEE Trans. Geosci. Electron.*, 1978, **GE-16**, 286–295.
29. Bernard, R., Martin, Ph, Thony, J. L., Vauclin, M. and Vidal-Madjar, D., C-band radar for determining surface soil moisture. *Remote Sensing Environ*., 1982, **12**, 189–200.